INFECTION AND IMMUNITY, Oct. 1997, p. 4299–4308 Vol. 65, No. 10
0019-9567/97/$04.00+0


# Hyperproduction, Purification, and Mechanism of Action of the Cytotoxic Enterotoxin Produced by *Aeromonas hydrophila*

M. R. FERGUSON, X.-J. XU, C. W. HOUSTON, J. W. PETERSON, D. H. COPPENHAVER, V. L. POPOV, AND A. K. CHOPRA*

*Department of Microbiology and Immunology, The University of Texas Medical Branch, Galveston, Texas 77555-1070*

Received 24 March 1997/Returned for modification 19 May 1997/Accepted 15 July 1997

**A gene encoding the cytotoxic enterotoxin (Act) from *Aeromonas hydrophila* was hyperexpressed with the pET, pTRX, and pGEX vector systems. Maximum toxin yield was obtained with the pTRX vector. Approximately 40 to 60% of Act was in a soluble form with the pTRX and pET vector systems. The toxin protein was purified to homogeneity by a combination of ammonium sulfate precipitation and fast protein liquid chromatography-based column chromatographies, including hydrophobic, anion-exchange, sizing, and hydroxylapatite chromatographies. Purified mature toxin migrated as a 52-kDa polypeptide on a sodium dodecyl sulfate (SDS)-polyacrylamide gel that reacted with Act-specific antibodies in immunoblots. The minimal amount of toxin needed to cause fluid secretion in rat ileal loops was 200 ng, and the 50% lethal dose for mice was 27.5 ng when injected intravenously. Binding of the toxin to erythrocytes was temperature dependent, with no binding occurring at 4°C. However, at 37°C the toxin bound to erythrocytes within 1 to 2 min. It was determined that the mechanism of action of the toxin involved the formation of pores in erythrocyte membranes, and the diameter of the pores was estimated to be 1.14 to 2.8 nm, as determined by the use of saccharides of different sizes and by electron microscopy. Calcium chloride prevented lysis of erythrocytes by the toxin; however, it did not affect the binding and pore-forming capabilities of the toxin. A dose-dependent reduction in hemoglobin release from erythrocytes was observed when Act was preincubated with cholesterol, but not with myristylated cholesterol. With $^{14}$C-labeled cholesterol and gel filtration, the binding of cholesterol to Act was demonstrated. None of the other phospholipids and glycolipids tested reduced the hemolytic activity of Act. The toxin also appeared to undergo aggregation when preincubated with cholesterol, as determined by SDS-polyacrylamide gel electorphoresis. As a result of this aggregation, Act's capacity to form pores in the erythrocyte membrane was inhibited.**

A cytotoxic enterotoxin gene (*act*) from the diarrheal isolate SSU of *Aeromonas hydrophila* was cloned and sequenced in our laboratory (9). The toxin protein (Act), which is 52 kDa in size, possesses hemolytic, cytotoxic, and enterotoxic activities and is lethal to mice when injected intravenously (37). Similar biological activities were reported for a hemolysin molecule which was isolated in 1984 by Asao et al. (1) from *A. hydrophila*. Subsequently, two aerolysin genes, one from a fish isolate of *A. hydrophila* (21, 22) and the other from a diarrheal isolate of *Aeromonas sobria* (8, 23), were cloned and sequenced. Chakraborty et al. (8) demonstrated that antibodies to the hemolysin isolated by Asao et al. reacted with their aerolysin on immunoblots (8). Comparison of the DNA and amino acid sequences of Act with those of an aerolysin from *A. sobria* revealed homologies of 76 and 79%, respectively. In contrast, homologies of 89 and 93% at the DNA and amino acid levels were detected between the aerolysin from a fish isolate and our Act (9, 22, 23). These data indicated that Act was an aerolysin-like molecule. However, the enterotoxic activity associated with aerolysin has not been examined. Amino acid compositional analysis of Act revealed that it differed from the more closely related aerolysin of a fish isolate at aspartyl, valyl, tyrosyl, and arginyl residues, which could result in differential folding of Act compared to aerolysin (22, 36). Our laboratory demonstrated all four biological activities with both the native Act purified from the diarrheal isolate SSU of *A. hydrophila* and the recombinant Act produced from *Escherichia coli.*

Recently, we identified regions on Act that were involved in the biological functions of the toxin by deletion analysis, by generating anti-peptide antibodies, and by site-directed mutagenesis (11). We also demonstrated that a synthetic peptide encompassing amino acid residues 245 to 274 of Act competed with the native toxin for receptor binding on Chinese hamster ovary (CHO) cells (11). The main focus of aerolysin's biological activity is its ability to lyse erythrocytes (13). However, our site-directed mutagenesis data indicated that alteration of some amino acid residues did not reduce or abrogate all three tested biological activities (i.e., hemolytic, cytotoxic, and enterotoxic) of Act (11). These data suggested for the first time that multiple biological activities of Act may be manifested by different loci on a single polypeptide chain of the toxin (11). Some amino acid residues (e.g., histidine [His$^{130}$ and His$^{155}$]) did not alter any of the tested biological activities of Act (11); however, substitution of analogous His residues appeared crucial for the hemolytic activity of aerolysin (13). Taken together, these data indicate that aerolysin-related toxins from different isolates of *Aeromonas* may possess structural and functional differences in addition to significant similarities. These differences could be significant with regard to the presence of specific biological activities, a conclusion consistent with the results of Asao et al. (2) in their characterization of two hemolysins from two different isolates (human and environmental) of *A. hydrophila*. We therefore opted to designate our toxin cytotoxic enterotoxin (Act) to differentiate it from aerolysin.

* Corresponding author. Mailing address: Department of Microbiology and Immunology, The University of Texas Medical Branch, Galveston, TX 77555-1070. Phone: (409) 747-0578. Fax: (409) 747-6869. E-mail: achopra@mspo6.med.utmb.edu.

Biological activities similar to that of the aerolysin-like molecule also were observed for a 36-kDa alpha-toxin of *Staphylococcus aureus*; however, the primary amino acid sequences of these molecules were completely unrelated (7). Blomquist and Sjorgen (7) reported that one monoclonal antibody generated to the alpha-toxin of *S. aureus* neutralized the lethal effect of the toxin but did not abrogate its hemolytic or dermonecrotic activity. These findings substantiate our results, implying that there could be different loci coding for various activities of Act. We have shown earlier that Act exhibited limited and scattered homology with the cytotoxin of *Pseudomonas aeruginosa*, the listeriolysin of *Listeria monocytogenes*, the enterotoxin of *Clostridium perfringens* type A, and the hemolysin of *E. coli* (11). Act undergoes processing at both the N- and C-terminal ends to demonstrate biological activity, as do aerolysin produced by *Aeromonas* species (8, 9, 19, 20), a cytotoxin elaborated by *P. aeruginosa* (16), and an alpha-toxin of *Clostridium septicum* (4, 38). Act has a leader sequence 23 amino acids long, which is removed when the toxin enters the periplasmic space (11). After the secretion of Act into the medium, an approximately 4- to 5-kDa polypeptide is cleaved from its C terminus by a protease produced by *A. hydrophila* SSU, resulting in the mature form of the toxin. However, in *E. coli* the hyperproduced Act was not secreted from the cells, and the precursor form of the toxin in the cell lysates could be processed in vitro into a biologically active form by trypsin treatment (11). Yamamoto and colleagues (42) reported that the cytolysin-hemolysin produced by *Vibrio cholerae* existed as an 82-kDa preprotoxin synthesized in the cytoplasm and secreted into the culture medium as a 79-kDa inactive protoxin after cleavage of the signal peptide. It was then processed into the 65-kDa active cytolysin by release of another N-terminal 15-kDa fragment (42).

We reported earlier the purification of Act from a wild-type *Aeromonas* culture (36). Although the toxin was purified to homogeneity, the yield of the purified toxin was less than 1%. The lack of sufficient quantities of purified toxin hampered our studies of the mechanism of action of this important virulence factor of *Aeromonas*. In this study, we report the hyperexpression of the *act* gene in *E. coli*, purification of the hyperproduced toxin and its mechanism of action, and the putative receptor of Act on erythrocytes.

## MATERIALS AND METHODS

**Bacterial strains and plasmids.** Isolate SSU of *A. hydrophila* was obtained from the Centers for Disease Control and Prevention, Atlanta, Ga. The DNA segment coding for the toxin gene (9) was amplified by PCR and ligated into the vector of choice at the 5′ *Xba*I and 3′ *Sal*I restriction sites. Essentially the protocol described by Perkin-Elmer Cetus (Norwalk, Conn.) was used for PCR. The PCR product was sequenced (3) with a Sequenase PCR sequencing kit (Amersham Life Sciences, Cleveland, Ohio) before it was subcloned into the expression vectors. The temperature-inducible *act* gene in expression plasmid vectors (pT7-5 and pT7-6) was used, as originally described by Tabor and Richardson (40). In expression plasmid pTRXFUS, the gene of interest was placed downstream and in frame with the thioredoxin gene (*trxA*) of *E. coli*, which is under the control of a tryptophan-inducible $\lambda p_L$ promoter (28). An enterokinase site separates TrxA from the protein of interest. In plasmid pGEX-KG, the *act* gene was placed downstream of the glutathione *S*-transferase (*gst*) gene, which is under the control of an isopropyl-β-D-thiogalactopyranoside (IPTG)-inducible *tac* promoter (14). A thrombin cleavage site separates the Gst from Act.

**DNA manipulations.** All of the DNA manipulations were performed as described in reference 3.

**Hyperexpression of the *act* gene.** We used essentially the method of Tabor and Richardson (40), as modified in our laboratory (34), to express the toxin gene with a bacteriophage T7 RNA polymerase-promoter system. Briefly, the *E. coli* (pGP1-2) recombinant clone (pT7-5*act*) was grown overnight at 30°C in a rich medium (39). The culture was induced at 42°C for 25 min, allowing expression of the bacteriophage T7 RNA polymerase gene. Rifampin (200 μg/ml) was then added to prevent endogenous RNA polymerase activity, and the culture was left at 42°C for an additional 10 min. The culture was then incubated for 2 h at 37°C. After sonication of the *E. coli* cells, the centrifuged cell lysate was used to measure the biological activities of the toxin. The recombinant *E. coli* GI724(pTRXFUS*act*) clone was grown at 30°C in M-9 induction medium (42 mM $Na_2HPO_4$, 22 mM $KH_2PO_4$, 9 mM NaCl, 19 mM $NH_4Cl$ [pH 7.4], 10 mM $MgSO_4$, 0.5% glucose, 0.1 mM $CaCl_2$, 0.2% casamino acids). At an optical density at 600 nm of 0.3, the culture was induced for 4 h by adding 100 μg of L-tryptophan/ml (Sigma, St. Louis, Mo.), and the temperature of the culture was shifted to 37°C (28). The cells were harvested, and the cell lysate was examined for various biological activities. With the pGEX-KG recombinant clone, the culture was grown at 37°C in Luria-Bertani medium. At an optical density at 600 nm of 0.3, the culture was induced with 1 mM IPTG and grown for another 4 h. The cell lysates were treated with 50 μg of trypsin (Gibco BRL, Grand Island, N.Y.)/ml for 1 h at 37°C to activate Act, and then trypsin inhibitor (Sigma) was added at a concentration of 0.1 mg/ml. The fusion proteins Gst-Act and TrxA-Act were cleaved with thrombin (Sigma) and enterokinase enzymes (Biozyme, San Diego, Calif.), respectively, as previously described (14, 28).

**Measurement of biological activity.** The biological activity of Act was measured by the lysis of rabbit erythrocytes (37), destruction of CHO cells, fluid secretory response in the rat ileal loop model (9), and a lethality test in mice (37). CHO cell destruction and lysis of erythrocytes were measured by determining the reciprocal of the highest dilution of Act required to cause 50% destruction of CHO cells or 50% lysis of erythrocytes. For enterotoxic activity, we injected different doses of Act in the ligated rat ileal loops (150 to 500 ng). The 50% lethal dose for the toxin was determined by the method of Reed and Muench (35), using six outbred Swiss Webster mice (Taconic Farms, Germantown, N.Y.) per group. The toxin was injected intravenously into the mice.

**Purification of Act.** Soluble Act was purified by the following protocol.

**(i) Ammonium sulfate precipitation.** The proteins in the clear cell lysate were precipitated by ammonium sulfate (60% saturation), dissolved in phosphate-buffered saline (PBS) (33) containing 1 mM phenylmethylsulfonyl fluoride, and ultracentrifuged at 100,000 × *g* for 2 h.

**(ii) Hydrophobic chromatography.** The biologically active sample (2.5 ml) in 1 M ammonium sulfate was subjected to fast protein liquid chromatography-based phenyl-Sepharose (1-ml bed volume; Pharmacia, Piscataway, N.J.) chromatography. After washing the column for 15 min with 1 M ammonium sulfate, we applied a linear gradient (50 min) of 1 M ammonium sulfate to distilled water. For the next 10 min, the column was washed with distilled water. The fractions (1 ml) were collected and assayed for hemolytic activity.

**(iii) Anion-exchange chromatography.** The biologically active fractions were concentrated, dialyzed against 0.05 M Tris-HCl (pH 7.5) plus 1 M urea, and loaded onto a Resource Q column (6-ml bed volume; Pharmacia). After the column was washed for 15 min, a linear gradient of 0.05 M Tris-HCl to 0.05 M Tris-HCl plus 0.5 M NaCl containing 1 M urea was developed (40 min), and the column was washed for another 10 min with a high-salt buffer.

**(iv) Molecular sizing.** After concentration, the pooled active fractions were chromatographed through two Superdex 75 columns (24-ml bed volume each; Pharmacia) connected in series. We loaded 500 μl of the sample for each run, and the fractions (1 ml) were collected for 76 min.

**(v) Hydroxylapatite chromatography.** The active pooled fractions were dialyzed against 10 mM potassium phosphate buffer (pH 6.8), and an aliquot (2.5 ml) of the sample was applied to a hydroxylapatite column (6-ml bed volume; Bio-Rad, Hercules, Calif.). The column was washed for 15 min, and then a linear gradient (30 min) of 10 mM to 500 mM phosphate buffer was applied. The column was washed for an additional 10 min with high-phosphate buffer, and the fractions were examined for biological activity.

**SDS-PAGE and Western blot analysis.** The hyperproduced toxin from different vector systems, as well as purified Act from various steps of purification, was analyzed by sodium dodecyl sulfate-polyacrylamide gel electrophoresis (SDS-PAGE) (10 to 12% polyacrylamide) (27). The gels were stained with either Coomassie blue or a silver-staining kit (Bio-Rad). The identity of Act was verified by immunoblot analysis with polyclonal affinity-purified antibodies (1 mg/ml) generated to the first 25 $NH_2$-terminal amino acid residues of Act. The monoclonal antibodies to the aerolysin from a fish isolate of *A. hydrophila*, Ah65, used in some Western blots were provided by J. T. Buckley (Department of Biochemistry and Microbiology, University of Victoria, Victoria, Canada). The secondary antibodies used were either goat anti-rabbit antibody conjugated with alkaline phosphatase or goat anti-mouse antibody conjugated with horseradish peroxidase (1:3,000). The blots were developed with the alkaline phosphatase conjugate substrate kit (Bio-Rad). Alternatively, the enhanced chemiluminescence substrate kit (Pierce, Rockford, Ill.) was used to develop the blots.

**Binding studies.** The rabbit erythrocytes (4%) were treated with 250 ng of the toxin for various periods of time (10 to 60 min) at 4 and 37°C. In binding and other mechanism of action studies, the final concentration of erythrocytes was 2%. The mixture of erythrocytes and toxin was then centrifuged at 4°C for 2 min, and the supernatant was examined for the release of hemoglobin at 540 nm (18). Inactive toxin (incubated at 65°C for 10 min) mixed with erythrocytes was used as a control in all mechanism of action experiments. The data from three independent experiments ± the standard error were plotted. When polyethylene glycol (PEG) 3350 (15 mM) was used in binding studies, it was added to 250 ng of Act along with 4% rabbit erythrocytes.

**Effect of saccharides on the release of hemoglobin.** Various saccharides (erythritol, xylose, arabinose, glucose, cellobiose, melibiose, raffinose, inulin, and PEG) in PBS (137 mM NaCl–3 mM KCl–0.68 mM $CaCl_2$–1 mM $CaCl_2 \cdot 2H_2O$–0.5 mM

TABLE 1. Purification of hyperproduced cytotoxic enterotoxin, originally from an isolate of *A. hydrophila*, with the pTRXFUS vector system

| Purification step | Total vol (ml) | Total protein[a] (mg) | Total hemolytic activity[b] | Specific activity[c] | Purification (fold) | % Recovery |
|---|---|---|---|---|---|---|
| Cell lysate | 62 | 9,563.5 | 126,976 | 13.2 | 1.0 | 100.0 |
| 60% $(NH_4)_2SO_4$ | 30 | 2,384.8 | 122,880 | 51.5 | 3.9 | 96.8 |
| Phenyl-Sepharose chromatography | 50 | 693.8 | 102,400 | 147.6 | 11.1 | 80.7 |
| Resource Q chromatography | 41 | 109.4 | 83,968 | 767.9 | 57.8 | 66.1 |
| Molecular sizing | 35 | 24.0 | 71,680 | 2,986.7 | 224.9 | 56.5 |
| Hydroxylapatite chromatography | 12 | 6.8 | 49,152 | 7,281.8 | 548.3 | 38.7 |

[a] Protein concentration was determined with the Bio-Rad protein assay kit.
[b] Hemolytic activity was defined as the reciprocal of the highest dilution of the toxin that exhibited 50% lysis of the rabbit erythrocytes.
[c] Specific activity was defined as the toxin activity per mg of protein.

$MgCl_2$ plus 8 mM $Na_2HPO_4$–15 mM $Na_2HPO_4 \cdot 7H_2O$–1.5 mM $KH_2PO_4$ [pH 7.4]) were mixed with Act (250 ng) and erythrocyte suspension (4%). The final concentration of most of the saccharides was 30 mM, but that of inulin and PEG was 15 mM. The mixture was incubated at 37°C for 1 h and then centrifuged before the release of hemoglobin was measured. The data from two independent experiments ± the standard error were presented.

**Effect of $CaCl_2$ on hemoglobin release.** Calcium chloride at various concentrations ranging from 0 to 300 mM (dissolved in 20 mM Tris–140 mM NaCl [pH 7.4]) was mixed with rabbit erythrocytes (4%) and Act (250 ng). The mixture was incubated at 37°C for 15 min and then centrifuged before the release of hemoglobin at 540 nm was measured.

**Effect of various lipids, phospholipids, and glycolipids on the release of hemoglobin.** Cholesterol and myristylated cholesterol (0 to 8 μg), phospholipids (phosphatidylethanolamine, phosphatidylinositol, phosphatidylglycerol, cardiolipin, phosphatidylcholine, phosphatidylserine, phosphatidic acid, and sphingomyelin; 8 and 16 μg), and glycolipids (mixed gangliosides; 8 and 16 μg) (Sigma) were mixed with Act (250 ng) and preincubated at 37°C for 15 min. After the preincubation, rabbit erythrocytes (4%) were added to the mixture and the incubation was continued at 37°C for 45 min. After centrifugation, the supernatant was examined for the release of hemoglobin at 540 nm.

**Binding of Act to $^{14}$C-labeled cholesterol.** Act (250 ng) was incubated with 2 μl (corresponding to 600 ng of cholesterol) of $^{14}$C-labeled cholesterol (specific activity, ~45 to 60 mCi/mmol; Dupont, Boston, Mass.) at 37°C for 30 min. The toxin-cholesterol mixture was then subjected to gel filtration with a Sephadex G-50 (Pharmacia) column (28 by 0.8 cm). Fifteen fractions (500 μl/microcentrifuge tube) were collected, and the radioactivity was measured in each fraction by using a Beckman LS 6000IC scintillation counter.

**Aggregation studies with Act, cholesterol, and erythrocytes.** Six microliters of Act (1 μg/ml), along with 3 μl of cholesterol (8 μg) and 41 μl of Tris-buffered saline (20 mM Tris–140 mM NaCl [pH 7.4]), was preincubated at 37°C for 30 min. After preincubation, 50 μl of rabbit erythrocytes (4%) was added, and the mixture was further incubated at 37°C for 40 min. The erythrocyte-toxin-cholesterol mixture was then centrifuged, and the pellet was resuspended in 65 μl of SDS-PAGE sample buffer (27). Thirty microliters of the sample was loaded onto a SDS–10% polyacrylamide gel, and the presence of toxin aggregates was examined by immunoblot analysis with toxin-specific antibodies. Act, erythrocytes without prior incubation with cholesterol, and cholesterol incubated with Act alone also were used in these experiments.

**Electron microscopy.** The rabbit erythrocyte ghosts were prepared by the procedure previously described by Dodge et al. (10). Ten microliters of erythrocyte ghost membranes (100 mM potassium phosphate buffer, pH 7.4), along with 5 μl (1 μg/ml) of toxin, was placed onto a Formvar-carbon coated copper grid and allowed to incubate at 37°C for 1 to 5 min. The toxin-membrane mixture was fixed with 2.5% glutaraldehyde in 0.1 M cacodylate buffer for 1 min, washed three times with $H_2O$ for 1 min, and negatively stained for 10 min with 2% phosphotungstic acid adjusted to pH 7.4 with 1 N KOH containing 0.2% sucrose. The specimens were observed under a Philips 201 transmission electron microscope at magnifications of $30 \times 10^3$ to $70 \times 10^3$. As a control, untreated erythrocyte ghost membranes were used throughout the experiment.

## RESULTS AND DISCUSSION

**Hyperexpression of the *act* gene.** The *act* gene was expressed with three different vector systems (pET, pTRXFUS, and pGEX), and significantly higher amounts of toxin antigen were produced with a pTRXFUS vector than with the pGEX-KG and T7 RNA polymerase-promoter systems. In the pGEX vector, a majority of the fusion protein was insoluble (data not shown). Act exists in two precursor forms, and processing at both the N-terminal (protoxin) and C-terminal (mature toxin) ends is required for manifestation of the biological activity of the toxin (9). Interestingly, a majority of the cytoplasmic fusion protein (TrxA-Act) was converted into protoxin (approximately 54 kDa) and a small portion was converted into an active toxin (52 kDa) by the action of *E. coli* protease(s), as was evident from Coomassie blue staining and immunoblot analysis (data not shown). The identities of the TrxA-Act (68 kDa), the protoxin (54 kDa), and the mature Act (52 kDa) were confirmed by N-terminal sequence analysis, in which the Coomassie blue-stained protein bands from the Immobilon-P membrane (Millipore, Bedford, Mass.) were sequenced directly. A significant portion of Act (60%) was associated with the membranes as an intact fusion protein (TrxA-Act) of 68 kDa, although some degradation and/or truncated products of Act were visualized on immunoblots. With the bacteriophage T7 RNA polymerase-promoter system, minimal degradation and/or truncation of the Act was noticed and approximately 60% of the toxin was present in a soluble form. However, the overall yield of the toxin was approximately 25% of that seen with the pTRXFUS vector (data not shown).

**Purification of the soluble Act.** The soluble form of Act was purified from the vector systems pET and pTRXFUS, with similar recoveries. The toxin protein was purified by a combination of ammonium sulfate precipitation and fast protein liquid chromatography-based chromatographies, based on hydrophobic interactions, charge, size, and an affinity to phosphate groups of hydroxylapatite matrix (Table 1). Most of the toxin was precipitated by 60% ammonium sulfate saturation. Upon chromatography on phenyl-Sepharose, the toxin was eluted with 100% water. The hydrophobic chromatography step resulted in an 11-fold purification of the toxin with 81% recovery (Table 1). On Resource Q chromatography, the toxin was eluted at 250 mM NaCl concentration, and this purification step resulted in a 58-fold purification and 66% cumulative recovery of the toxin (Table 1). When the biologically active pool was sized on the Superdex 75 column, we detected two major protein peaks, and the biological activity was associated with the second peak. Finally, the toxin was purified to homogeneity by hydroxylapatite chromatography, and the toxin protein was eluted as a sharp peak at 245 mM potassium phosphate concentration. Overall, a 548-fold purification and 38% recovery of the toxin were achieved (Table 1). It is worth mentioning that all of the pooled and concentrated fractions were treated with trypsin after various purification steps to convert the precursor form of the toxin into an active Act (11). The efficiency of the trypsin treatment was monitored by SDS-PAGE and immunoblot analysis (Fig. 1b, lane 2). Routinely, a four- to eightfold increase in the hemolytic activity was observed after trypsin treatment. The purification of the toxin during various biochemical steps is depicted in Fig. 1a and c.

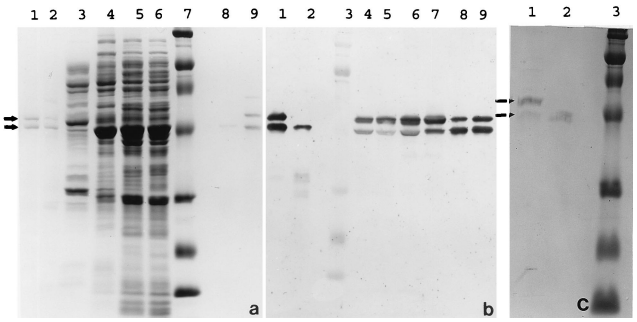


FIG. 1. SDS-PAGE of the *E. coli* cell lysates containing TrxA-Act during different purification stages. (a) Coomassie blue-stained gel. Lanes 1 to 8 contain toxin preparations after various chromatography steps. Pure toxin (2 μg) is shown after hydroxylapatite chromatography (lane 1); after sizing (Superdex 75) (lanes 2 and 9); after resource Q chromatography (lane 3); after hydrophobic chromatography (phenyl-Sepharose) (lane 4); after ammonium sulfate precipitation (60% saturation) (lane 5); and after trypsin treatment of the toxin from lane 1 (lane 8). Lane 6, crude cell lysate (starting material); lane 7, rainbow marker (Amersham). (b) Western blot analysis with anti-peptide antibodies to Act. Pure toxin is shown after hydroxylapatite chromatography (lanes 1 and 9); after trypsin treatment (lane 2); after ammonium sulfate precipitation (60% saturation) (lane 5); after hydrophobic chromatography (phenyl-Sepharose) (lane 6); after Resource Q chromatography (lane 7); and after sizing (Superdex 75) (lane 8). Lane 3 contains marker and lane 4 contains crude cell lysate (starting material). (c) Coomassie blue-stained gel. Lane 1, pure toxin (4 μg) before trypsin treatment; lane 2, pure toxin (4 μg) after trypsin treatment; lane 3, rainbow marker. The arrows represent the precursor form (54 kDa) and the mature form (52 kDa) of Act.

Lanes 1 in Fig. 1a and c show the toxin protein after hydroxylapatite chromatography. Two protein bands represent the precursor (54 kDa) and the smaller (52 kDa), mature form of the toxin. After digestion with trypsin, the precursor form of the toxin was converted into an active form (Fig. 1a, lane 8, and c, lane 2). The identity of these polypeptides was confirmed by N-terminal sequence analysis, and the purity of Act was also examined by silver staining of the gels.

**Toxin dose required for various biological activities.** The availability of the purified toxin allowed us to perform dose-response studies to determine the minimum amount of the toxin required to cause a fluid secretory response in the rat ileal loop assay. The minimum concentration of the toxin needed to cause fluid secretion during a 12-h observation period was approximately 200 ng (0.3 to 0.4 ml/cm of the loop). However, a lower dose (150 to 175 ng) resulted in no fluid secretion. The 50% lethal dose for mice was calculated to be 27.5 ng. The minimum Act doses required for 50% lysis of erythrocytes and to cause the destruction of CHO cells (50%) were 200 ng and 62 pg, respectively.

**Temperature-dependent binding of the toxin to erythrocytes.** Our data indicated that binding of the toxin to the erythrocytes was temperature dependent. When erythrocytes were incubated with the toxin at 4°C for 60 min, there was no detectable release of hemoglobin (data not shown). However, when the same reaction mixture was incubated at 37°C for various periods, a significant amount of hemoglobin was released within the first 20 min of incubation (Fig. 2A). To further demonstrate that the binding of the toxin was temperature dependent, the erythrocytes were incubated with the toxin at 4°C for 1 h. Subsequently, the cells were washed three times with cold PBS and the erythrocytes were resuspended in PBS with toxin (250 ng) and without toxin (Fig. 2B). The logic was that if the toxin did not bind to the erythrocytes at 4°C, then washing of the erythrocytes would remove all of the unbound toxin. Therefore, further incubation of the reaction mixture at 37°C would not show any detectable release of hemoglobin. Binding of the toxin to the erythrocytes did not occur at 4°C, because when the toxin was removed, no hemolytic activity was demonstrated, even at 37°C. However, in the control experiment, in which the toxin remained in contact with the erythrocytes both at 4 and 37°C, a significant release of hemoglobin was noticed at 37°C (Fig. 2B), indicating clearly that the binding of the toxin to the erythrocytes occurred at 37°C but not at 4°C. In contrast, the binding of the hemolysin

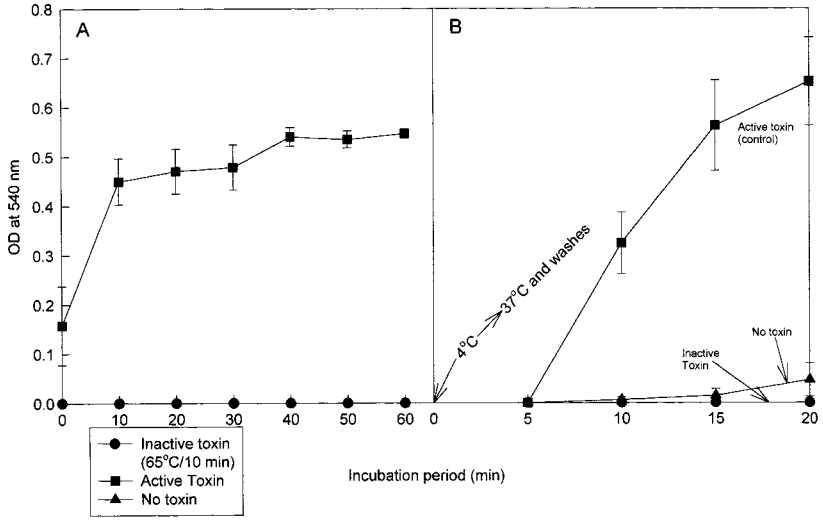


FIG. 2. Effect of temperature on the hemolytic activity of Act and its binding to erythrocytes. (A) The toxin-erythrocyte mixture was incubated at 37°C, and the release of hemoglobin at various time intervals was examined. The release of hemoglobin at different time points was statistically significant compared to the control (0-min sample) by Student's *t* test ($P < 0.05$). (B) Binding of the toxin to erythrocytes is temperature dependent. After incubation at 4°C for 60 min, the toxin-erythrocyte mixture was pelleted, washed three times with PBS, and resuspended in PBS without toxin and with toxin (250 ng) at 37°C. The arrow at time zero indicates the change in temperature from 4 to 37°C. The reaction mixture was incubated at 37°C for up to 20 min. The release of hemoglobin with and without toxin was statistically significant by Student's *t* test ($P < 0.05$). OD, optical density.

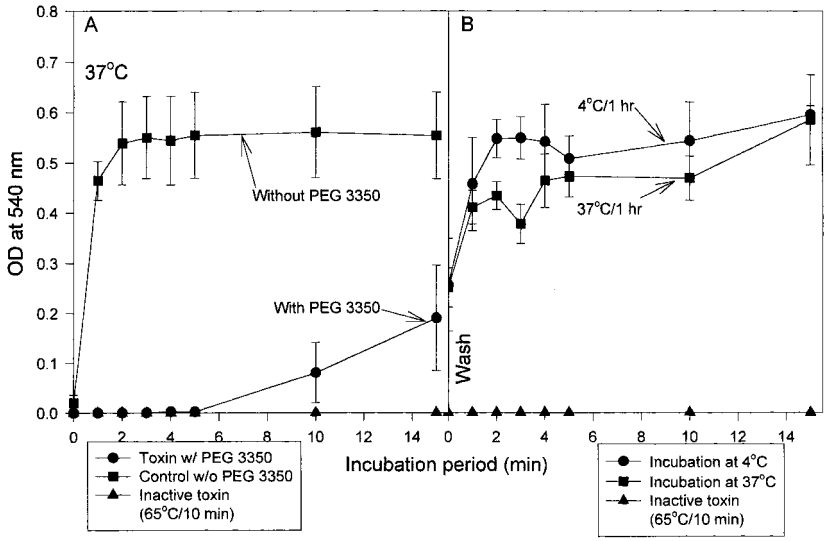


FIG. 3. PEG prevents the lysis of erythrocytes but not the binding of the toxin to the erythrocytes. The toxin-erythrocyte-PEG 3350 mixture was incubated at 37°C for various periods of time up to 15 min (A), washed three times with PBS, resuspended in PBS without the toxin and PEG, and incubated at 4 or 37°C for 1 h (B). The toxin-erythrocyte mixture without PEG 3350 also was used as a control to demonstrate normal lysis of erythrocytes (A). The release of hemoglobin at different time points in the absence of PEG was statistically significant compared to the 0-min control by Student's *t* test ($P < 0.05$). The release of hemoglobin in the presence of PEG was statistically insignificant ($P > 0.05$) when compared at different time intervals. Furthermore, the release of hemoglobin without PEG was statistically significant ($P < 0.05$) when compared to the release of hemoglobin with PEG (A). The release of hemoglobin at 4 and 37°C was statistically insignificant ($P > 0.05$) (B). OD, optical density.

of *Vibrio vulnificus* (25), the alpha-toxin of *C. septicum* (38), perfringolysin O of *C. perfringens* (15), and the cytolysin of *V. cholerae* (24) to erythrocytes was temperature independent. The hemolysin of *Vibrio parahaemolyticus* (18) bound to the membranes of erythrocytes in a temperature-dependent manner, like Act, with binding occurring only at 37°C.

To determine the time required by Act to bind to erythrocytes at 37°C, we mixed the toxin-erythrocyte mixture with PEG 3350 (15 mM), which prevented lysis of erythrocytes (see next section), for various periods of time (0 to 15 min) at 37°C (Fig. 3A). The mixture was then centrifuged, and the erythrocytes were resuspended in cold PBS without toxin and PEG. The cells were then incubated at either 4 or 37°C for 1 h (Fig. 3B). It is evident that initial exposure of the toxin to the erythrocytes at 37°C for 1 to 5 min caused the same release of hemoglobin as in the sample which was exposed at 37°C for 15

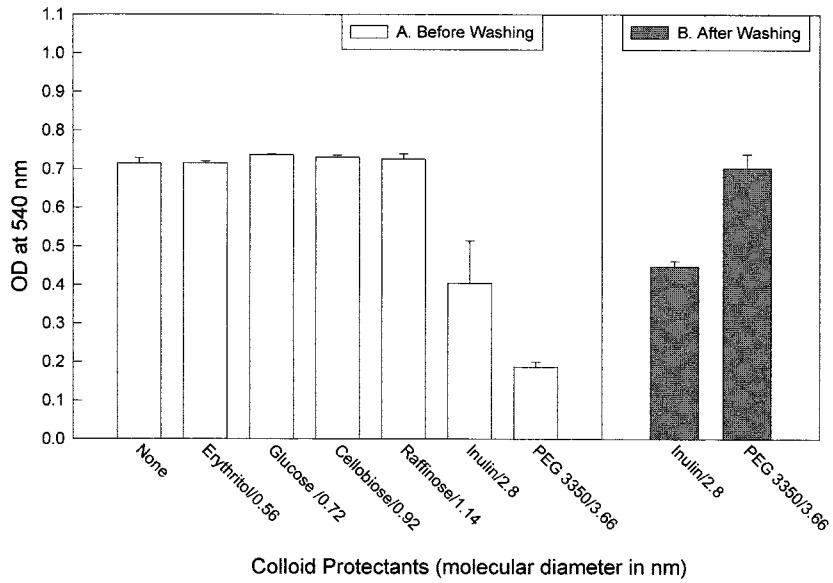


FIG. 4. Inhibitory effects of saccharides on cytotoxic enterotoxin-induced hemolysis. (A) Act (250 ng) was mixed with different saccharides, 4% rabbit erythrocytes was added, and the mixture was incubated at 37°C for 1 h. (B) The mixture of saccharides (inulin, PEG 3350, and PEG 6000), toxin, and erythrocytes was washed once with PBS, and the hemoglobin released in the PBS was measured at 540 nm. The release of hemoglobin with inulin, PEG 3350, and PEG 6000 was statistically significant by Student's *t* test ($P < 0.05$) when compared with the control in panel A. The release of hemoglobin shown in panel B was statistically insignificant ($P > 0.05$) by Student's *t* test when compared to the control in panel A. Error bars indicate standard deviations. OD, optical density.

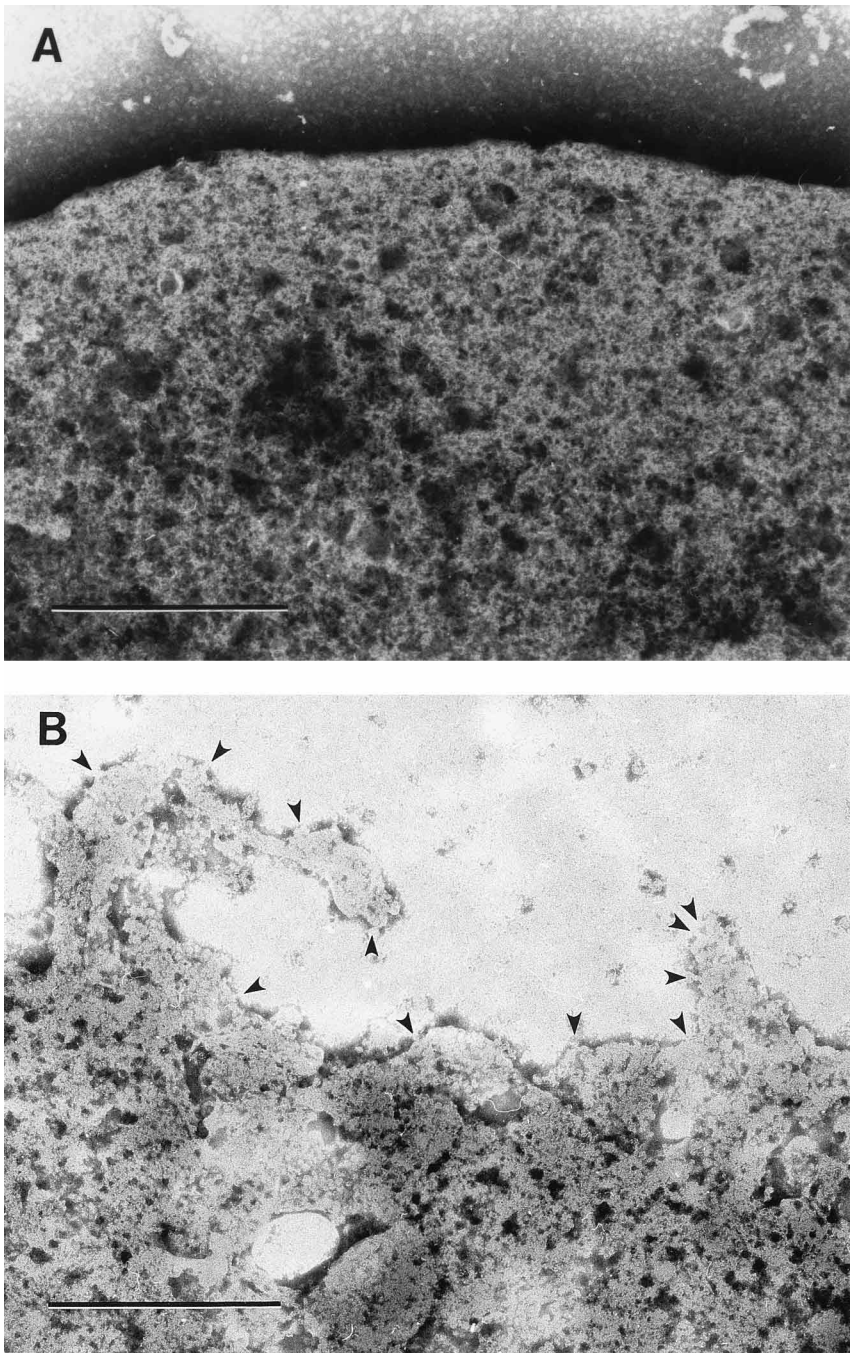


FIG. 5. Electron microscopy demonstrates the presence of pores on erythrocyte membranes. (A) Untreated erythrocyte ghost membranes were used throughout the experiment as a control. (B) Rabbit erythrocyte ghosts along with toxin were incubated at 37°C for 5 min on a copper grid. The toxin-membrane mixture was fixed and washed, and the samples were subjected to negative staining. The specimens were observed under an electron microscope. Arrowheads indicate the pores created in the membrane. Bars, 0.5 μm.

min (Fig. 3A). These data indicated that the binding of the toxin to the erythrocytes was rapid and that once the toxin was bound to the erythrocytes, the hemolysis proceeded in a similar fashion at both 4 and 37°C (Fig. 3B).

**Hole formation in the erythrocytes by the toxin.** Our earlier studies with $^{51}Cr$ indicated that Act caused a rapid release of $^{51}Cr$ from CHO cells (37). To further confirm that this release of $^{51}Cr$ was due to the ability of Act to form pores in the membrane, we conducted the following studies. The toxin was mixed with different saccharides for which the diameter of the particle was known. Erythrocytes were added to the mixture, and the suspension was incubated at 37°C for 1 h (Fig. 4A). It is evident that when we used sugars, such as erythritol, xylose, arabinose, glucose, cellobiose, melibiose, and raffinose, which have a particle diameter in the range of 0.56 to 1.14 nm, the lysis of the erythrocytes proceeded in a manner similar to that of the controls to which no saccharide was added. The mechanism of action of the toxin may involve entry of water from

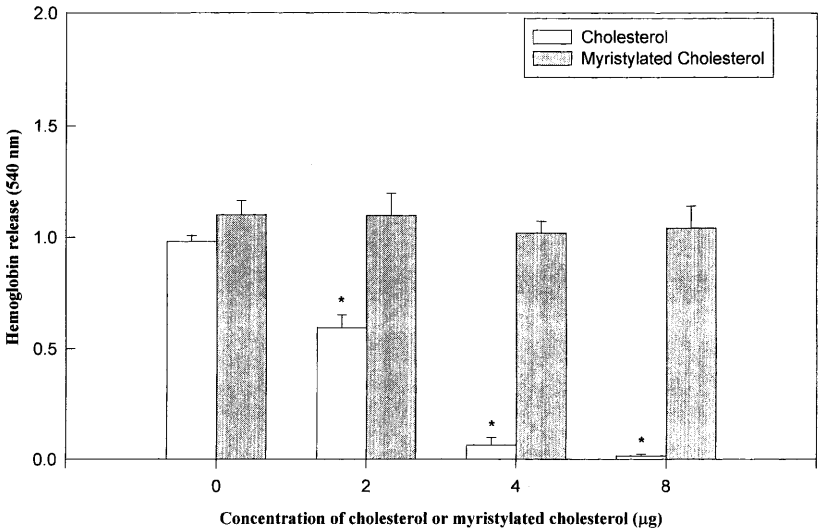


FIG. 6. Effect of cholesterol and myristylated cholesterol on Act-induced hemolysis. Two hundred microliters each of cholesterol and myristylated cholesterol at various concentrations ranging from 0 to 8 μg were mixed with 200 μl of the toxin (250 ng) and preincubated at 37°C for 15 min. After the preincubation, 400 μl of rabbit erythrocytes (4%) was added and the mixture was incubated at 37°C for 45 min before the release of hemoglobin at 540 nm was measured. The data represent an average of three independent experiments ± the standard error. Asterisks indicate that results were statistically significant by Student's *t* test ($P < 0.05$) when compared to the control.

the external milieu into erythrocytes through the pores created by the toxin, resulting in swelling of the cells and subsequent lysis. Since sugars with a particle diameter in the range of 0.56 to 1.14 nm did not affect the lysis of erythrocytes, the size of the pores created by the toxin was larger than 1.14 nm. Partial hemolysis of erythrocytes occurred when inulin (2.8-nm particle diameter) was used. When PEG (diameter, 3.66 to 5.66 nm) was added to the erythrocyte-toxin mixture, the blood cells did not lyse, as indicated by the lack of hemoglobin release (Fig. 4A). These data indicated that the size of the pores was in the range of 1.14 to 2.8 nm. Like our toxin, many other bacterial toxins interact with the membranes of target cells, insert into the lipid bilayer as oligomers, and create pores in the range of 0.92 to 3 nm. These toxins include the aerolysin of *A. hydrophila* and *A. sobria* (19), *V. parahaemolyticus* hemolysin (18), an *E. coli* hemolysin (5), a staphylococcal alpha-toxin (6), and cytolysins of *V. cholerae* and *V. vulnificus* (24, 25).

We washed the toxin-erythrocyte-saccharide-treated mixture with PBS (3×), resuspended the components in toxin- and saccharide-free cold PBS, and incubated the mixture further at 37°C for 1 h to demonstrate that inulin and PEG did not inhibit erythrocyte lysis because they prevented toxin from binding to erythrocytes. As shown in Fig. 4B, normal lysis of the erythrocytes occurred, indicating that the toxin did bind to the erythrocytes and that certain saccharides (e.g., inulin and PEG) increased the osmotic pressure in the external milieu, resulting in the osmotic stabilization of the erythrocytes.

The pore formation by Act on the erythrocyte membrane was confirmed further by electron microscopy as shown in Fig. 5. The toxin-treated membranes showed an uneven surface texture (Fig. 5B), whereas the control (no toxin treatment) had a relatively smooth surface (Fig. 5A). Numerous gaps, suggestive of pores, existed throughout the toxin-treated membranes. The pore sizes ranged from 10 to 13 nm, which was larger than that calculated from the osmotic protection assays (1.14 to 2.8 nm). This discrepancy may be attributed to the fact that the saccharide protectant experiments measure the pore diameter at the most constricted area, whereas electron microscopy observes only the external orifice of the pore. A similar discrepancy was reported for the hemolysin of *V. parahaemolyticus*, in which the pore size ranged from 30 to 35 nm by electron microscopy and measured 2 nm by the colloidal protection assay (18). In the hemolysin of *V. cholerae*, the pore size was 4 nm by electron microscopy and 1.2 to 1.6 nm in the colloidal protection assay (24). Furthermore, the processing of the specimens for electron microscopy also might have affected the pore size (24).

**Inhibitory effect of calcium on Act-induced hemolysis of erythrocytes.** We examined the effect of $Ca^{2+}$ on the hemolytic activity of Act in order to understand further the mechanism of action. Calcium in a millimolar concentration range (100 to 300 mM) prevented lysis of rabbit erythrocytes, with 80% protection at 200 mM $CaCl_2$ concentration (data not shown). We incubated the toxin with erythrocytes and 200 mM $CaCl_2$ at 37°C for 25 min to determine whether the binding of the toxin to the membranes of erythrocytes was affected by $CaCl_2$. After centrifugation, toxin-bound erythrocytes were washed in a medium without $Ca^{2+}$ and incubation was continued at 37°C for 5 min. Under these conditions, the protective effect of $Ca^{2+}$ was lost and the cells proceeded to lyse in a manner comparable to that of the control, indicating that $Ca^{2+}$ did not interfere with the binding of Act to erythrocytes (data not shown).

We then examined the effect of $Ca^{2+}$ on pore formation. After 25 min of incubation at 37°C of the toxin with erythrocytes and 200 mM $CaCl_2$, the mixture was centrifuged and the cells were suspended in Tris-NaCl containing 200 mM $CaCl_2$. Our data indicated that the inhibitory effect of $Ca^{2+}$ on erythrocytes persisted. However, when this same sample was washed once with medium without $Ca^{2+}$, the release of hemoglobin was observed. These data strongly suggested that calcium ions did not interfere with the ability of Act to bind and form pores. A possible explanation for the inhibitory effect of $Ca^{2+}$ is that it caused changes in the rigidity of the erythrocyte membranes such that the hemoglobin could not be released. The role of $Ca^{2+}$ in binding and pore formation by *E. coli* hemolysin with the erythrocytes has been reported in the literature (29). However, our results indicated that $Ca^{2+}$ prevented the lysis of erythrocytes. Similarly, van Leengoed and Dickerson (41) re-

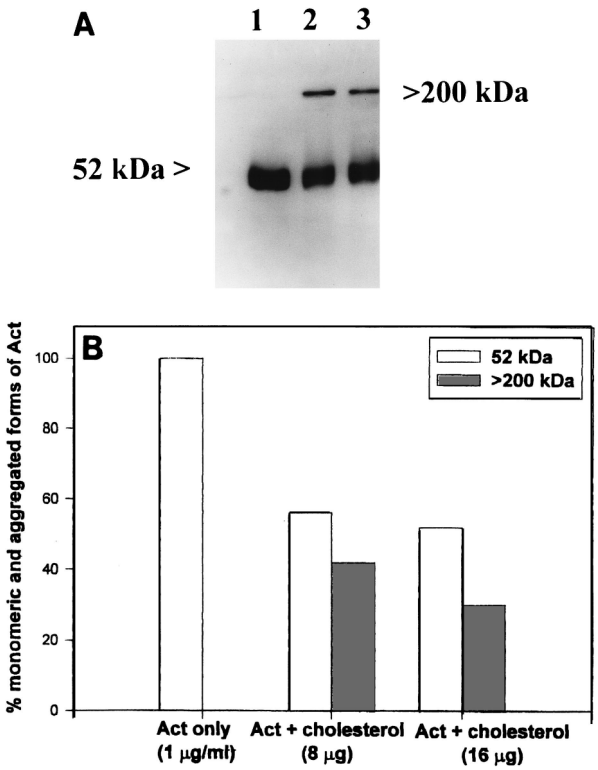


FIG. 7. SDS-PAGE and immunoblot analysis demonstrate aggregation of Act. Act along with cholesterol was allowed to preincubate at 37°C for 30 min. After preincubation, rabbit erythrocytes were added and the mixture was further incubated at 37°C for 40 min. (A) Lane 1, Act only (1 μg/ml); lane 2, Act plus cholesterol (8 μg); lane 3, Act plus cholesterol (16 μg). (B) The amount of protein in each lane was quantitated by densitometer scanning (Applied Imaging, Pittsburgh, Pa.) of the bands.

ported that hemolytic activity associated with *Actinobacillus pleuropneumoniae* hemolysin as well as the binding of this toxin to erythrocytes was dependent on $Ca^{2+}$. Kraut and colleagues (26) noted that the postbinding programming for the lysis of natural killer cell-mediated cytolysis was $Ca^{2+}$ dependent. They suggested that the $Ca^{2+}$ dependency of cytolysin-mediated cytolysis is related to increases in intracellular $Ca^{2+}$. Miyake et al. (31) demonstrated that divalent cations, such as $Cd^{2+}$, $Cu^{2+}$, $Ni^{2+}$, $Sn^{2+}$, and $Zn^{2+}$, inhibited the hemolysis of rabbit erythrocytes caused by *Vibrio metschnikovii* cytolysin. We intend to examine the effects of other divalent cations on the binding and pore formation of Act with erythrocyte membranes.

**The nature of *Aeromonas* Act receptor.** None of the phospholipids and glycolipids tested at concentrations of 8 and 16 μg/800 μl of the reaction mixture reduced the hemolytic activity of Act (250 ng) as measured by the release of hemoglobin (0.928 ± 0.144 to 1.08 ± 0.285 and 1.134 ± 0.082 for phospholipids and glycolipids, respectively). The release of hemoglobin from erythrocytes by Act alone was 1.02 ± 0.212. We observed a dose-dependent reduction in hemoglobin release with cholesterol but not with myristylated cholesterol (Fig. 6). The hydroxyl group of cholesterol is modified in myristylated cholesterol. Therefore, it appears that the hydroxyl group associated with cholesterol may be important for the interaction of toxin with this membrane constituent. Alternatively, the effect of cholesterol may be incompatible with the fatty acid tail in myristylated cholesterol, which may dramatically change its properties. This could result in myristylated cholesterol having no effect on the hemolytic activity of Act. Once Act interacted with cholesterol on the membranes of erythrocytes, aggregation of Act occurred, which was demonstrated by immunoblot analysis (Fig. 7). Consequently, this process induced cytolysis by osmotic swelling of the cell. Act underwent aggregation to the same extent when mixed with cholesterol whether or not erythrocytes were present. Act-specific antibodies did not exhibit any reaction with cholesterol and erythrocyte membrane proteins in immunoblots (data not shown). Thus, the presence of exogenous cholesterol was not necessary for Act to undergo multimerization, and the presence of erythrocyte membranes was sufficient to mediate this effect. The ability of cholesterol to affect the biological activity of Act indicated that either cholesterol served as the receptor for Act or it induced multimerization of the toxin, leading to its loss of biological activity.

We measured the association of $^{14}C$-labeled cholesterol with Act by gel filtration to demonstrate that Act was bound to cholesterol. Our data indicated that Act, which is 52 kDa in size, eluted in the void volume of the Sephadex G-50 column. However, free cholesterol, which is very small (approximately 400 Da) and lipid in nature, did not elute even after extensive washing of the column with PBS (20 bed volumes). In contrast, when the toxin was mixed with the $^{14}C$-labeled cholesterol, a significant portion of the labeled cholesterol (73% ± 18%; $n$ = 7) was eluted with the toxin in the void volume, clearly indicating that Act was bound to cholesterol. The hemolytic activity of Act in these experiments was reduced by 76% after being mixed with cholesterol (600 ng). Ikigai et al. (24) reported that cholesterol was essential for the oligomerization of *V. cholerae* O1 El Tor hemolysin. Earlier, Garland and Buckley (12) indicated that the interaction of aerolysin with rat erythrocytes suggested that the receptor was the major membrane glycoprotein that migrated at 79 kDa and that it corresponded to human glycophorin. However, Hermann et al. (17) recently reported the partial purification of the rat erythrocyte receptor for aerolysin produced by *A. hydrophila*. They demonstrated that the receptor was a 47-kDa glycoprotein which was sensitive to proteases and *N*-glycosidase. They further suggested that the inhibition of aerolysin-induced hydrolysis with human glycophorin might have occurred because the toxin formed micelles in solution when mixed with glycophorin (17). The negatively charged surface of glycophorin could bind to aerolysin, resulting in its oligomerization and the inactivation of the toxin's biological activity. However, our studies indicated that glycophorin was not the receptor for Act, since no reduction in Act's biological activity was noticed when it was preincubated with human glycophorin (25 to 100 μg) (Sigma). The aerolysin receptor has some intriguing similarities to the *P. aeruginosa* cytolysin-binding protein of rabbit erythrocytes, which has been reported to be 43 to 60 kDa in size (17). Lutz et al. (30) reported that this glycoprotein corresponded to the integral protein CHIP28, which formed a water channel in the human erythrocyte membrane. The conclusion that the mode of action of *P. aeruginosa* cytolysin may not be to form its own channels but to control the opening or closing of an existing channel has been elucidated.

The toxin (Act) aggregate, once formed, was stable to heating and to the effect of SDS and 2-β-mercaptoethanol (Fig. 7), unlike the El Tor hemolysin produced by *V. cholerae* O1 (24). On the other hand, Zitzer et al. (43) reported recently that the *V. cholerae* El Tor cytolysin oligomers were stable to boiling in SDS. Similarly, Nakamura et al. (32) demonstrated that perfringolysin O, produced by gram-positive *C. perfringens* type A, bound specifically to membrane cholesterol, forming oligomeric pores that were stable in the presence of SDS, as Act is.

Based on the recent three-dimensional studies on the alpha-hemolysin of *S. aureus*, it is clear that the toxin forms heptamers to create pores (39). The structure elucidates the heptameric subunit stoichiometry of the alpha-hemolysin oligomer and shows that a glycine-rich and solvent-exposed region of a water-soluble protein can self-assemble to form a transmembrane pore of defined structure. The membrane-bound monomers assemble to form 232.4-kDa heptameric transmembrane pores. The heptamer is the cytolytic species, and the primary mechanism of cell death involves the bilayer permeabilization to ions, water, and low-molecular-weight molecules; disruption of the cellular osmotic balance; and ultimately cell lysis. The structure of the pore-forming domain of the alpha-hemolysin may define a more accurate model for the structure of Act and other related pore-forming toxins.

In conclusion, we have hyperproduced the cytotoxic enterotoxin originally cloned from *A. hydrophila*, which allowed us to study the mechanism of action of this important virulence factor. The purified toxin will allow us to generate monoclonal antibodies, which can be used in mapping epitopes on Act that are involved in receptor binding on the eukaryotic cells and in the manifestation of various biological activities of the toxin. In general, there seem to be some common mechanisms of pore formation by toxins produced by gram-negative and gram-positive organisms. Act clearly exhibits differences with and similarities to other pore-forming toxins produced by members of the families *Vibrionaceae* and *Enterobacteriaceae*. These data suggest that various pore-forming toxins have originated by divergent evolution over time, maintaining similar mechanisms of action but diverging significantly in their primary amino acid sequences. In these studies, we have also demonstrated the putative receptor on erythrocytes to which Act binds. However, more studies are needed to conclusively prove that cholesterol is the major receptor for Act. It will be intriguing to create, by site-directed mutagenesis, a mutated toxin which can still undergo aggregation but which will not cause lysis of the cells in order to determine whether additional steps in the lytic process exist between aggregation and the lysis of erythrocytes. The molecular basis for transmembrane pore formation for gram-negative organisms awaits resolution in the future.

## ACKNOWLEDGMENTS

This work was supported in part by grant R01AI41611 from the National Institutes of Health and a recruitment grant from the John Sealy Endowment Fund for Biomedical Research, UTMB, Galveston, Tex. M.R.F. is supported by a McLaughlin predoctoral fellowship.

We thank Mardelle Susman for editorial comments and Kevin Hood McKinney for designing the graphs for the mechanism of action studies. We also thank Elena Aguiluz, an ASM undergraduate research fellow, for conducting the $^{14}$C-labeled cholesterol experiments and Antonio Duran for participating in the mechanism of action studies.

## REFERENCES

1. **Asao, T., Y. Kinoshita, S. Kozaki, T. Uemura, and G. Sakaguchi.** 1984. Purification and some properties of *Aeromonas hydrophila* hemolysin. Infect. Immun. **46:**122–127.
2. **Asao, T., S. Kozaki, K. Kato, Y. Kinoshita, K. Otsu, T. Uemura, and G. Sakaguchi.** 1986. Purification and characterization of an *Aeromonas hydrophila* hemolysin. J. Clin. Microbiol. **24:**228–232.
3. **Ausubel, F. M., R. Brent, R. E. Kingston, D. D. Moore, J. Seidman, J. A. Smith, and K. Struhl (ed.).** 1989. Current protocols in molecular biology. John Wiley and Sons, Inc., New York, N.Y.
4. **Ballard, J., J. Crabtree, B. A. Roe, and R. K. Tweten.** 1995. The primary structure of *Clostridium septicum* alpha-toxin exhibits similarity with that of *Aeromonas hydrophila* aerolysin. Infect. Immun. **63:**340–344.
5. **Bhakdi, S., N. Mackman, M. J. Nicaud, and I. B. Holland.** 1986. *Escherichia coli* hemolysin may damage target cell membranes by generating transmembrane pores. Infect. Immun. **52:**63–69.
6. **Bhakdi, S., M. Muhly, and R. Füssle.** 1984. Correlation between toxin binding and hemolytic activity in membrane damage by staphylococcal α-toxin. Infect. Immun. **46:**318–323.
7. **Blomquist, L., and A. Sjorgen.** 1988. Production and characterization of monoclonal antibodies against *S. aureus* alpha toxin. Toxicon **26:**265–273.
8. **Chakraborty, T., B. Huhle, H. Bergbauer, and W. Goebel.** 1986. Cloning, expression, and mapping of the *Aeromonas hydrophila* aerolysin gene determinant in *Escherichia coli* K-12. J. Bacteriol. **167:**368–374.
9. **Chopra, A. K., C. W. Houston, J. W. Peterson, and G. F. Jin.** 1993. Cloning, expression, and sequence analysis of a cytolytic enterotoxin gene from *Aeromonas hydrophila*. Can. J. Microbiol. **39:**513–523.
10. **Dodge, J. T., C. Mitchell, and D. J. Hanahan.** 1963. The preparation and chemical characteristics of hemoglobin-free ghosts of human erythrocytes. Arch. Biochem. Biophys. **100:**119–130.
11. **Ferguson, M. R., Xin-Jing Xu, C. W. Houston, J. W. Peterson, and A. K. Chopra.** 1995. Amino-acid residues involved in biological functions of the cytolytic enterotoxin from *Aeromonas hydrophila*. Gene **156:**79–83.
12. **Garland, W. J., and J. T. Buckley.** 1988. The cytolytic toxin aerolysin must aggregate to disrupt erythrocyte membranes, and aggregation is stimulated by human glycophorin. Infect. Immun. **56:**1249–1253.
13. **Green, M. J., and J. T. Buckley.** 1990. Site-directed mutagenesis of the hole-forming toxin aerolysin: studies on the roles of histidines in receptor binding and oligomerization of the monomer. Biochemistry **29:**2177–2180.
14. **Guan, K., and J. E. Dixon.** 1991. Eukaryotic proteins expressed in *E. coli*: an improved thrombin cleavage and purification procedure of fusion proteins with glutathione *S*-transferase. Anal. Biochem. **192:**262–267.
15. **Harris, R. W., P. J. Sims, and R. K. Tweten.** 1991. Kinetic aspects of the aggregation of *Clostridium perfringens* O-toxin on erythrocyte membranes. J. Biol. Chem. **266:**6936–6941.
16. **Hayashi, T., Y. Kamio, F. Hishinuma, U. Usami, K. Titani, and Y. Terawaki.** 1989. *Pseudomonas aeruginosa* cytotoxin: the nucleotide sequence of the gene and the mechanism of action of the protoxin. Mol. Microbiol. **3:**861–868.
17. **Hermann, J. G., H. U. Wilmsen, S. Cowell, H. Schindler, and J. T. Buckley.** 1994. Partial purification of the rat erythrocyte receptor for channel-forming toxin aerolysin and reconstitution into planar lipid bilayers. Mol. Microbiol. **14:**1093–1101.
18. **Honda, T., N. Yuxin, and T. Miwatani.** 1992. The thermostable direct hemolysin of *Vibrio parahaemolyticus* is a pore-forming toxin. Can. J. Microbiol. **38:**1175–1180.
19. **Howard, P., and J. T. Buckley.** 1982. Membrane glycoprotein receptor and hole-forming properties of a cytolytic protein toxin. Biochemistry **21:**1662–1667.
20. **Howard, S. P., and J. T. Buckley.** 1985. Activation of the hole-forming toxin aerolysin by extracellular processing. J. Bacteriol. **163:**336–340.
21. **Howard, S. P., and J. T. Buckley.** 1986. Molecular cloning and expression in *Escherichia coli* of the structural gene for the hemolytic toxin aerolysin from *Aeromonas hydrophila*. Mol. Gen. Genet. **204:**289–295.
22. **Howard, S. P., W. J. Garland, M. J. Green, and J. T. Buckley.** 1987. Nucleotide sequence of the gene for the hole-forming toxin aerolysin of *Aeromonas hydrophila*. J. Bacteriol. **169:**2869–2871.
23. **Husslein, V., B. Huhle, T. Jarchau, R. Lurz, W. Goebel, and T. Chakraborty.** 1988. Nucleotide sequence and transcriptional analysis of the *AerCaerA* region of *Aeromonas sobria* encoding aerolysin and its regulatory region. Mol. Microbiol. **2:**507–517.
24. **Ikigai, H., A. Akatsuka, H. Tsujiyama, T. Nakae, and T. Shimamura.** 1996. Mechanism of membrane damage by El Tor hemolysin of *Vibrio cholerae* O1. Infect. Immun. **64:**2968–2973.
25. **Kim, H.-R., H.-W. Rho, M.-H. Jeong, J.-W. Park, J.-S. Kim, B.-H. Park, U.-H. Kim, and S.-D. Park.** 1993. Hemolytic mechanism of cytolysin produced from *V. vulnificus*. Life Sci. **53:**571–577.
26. **Kraut, R. P., R. Bose, E. J. Cragoe, and A. H. Greenberg.** 1992. The $Na^+/Ca^{2+}$ exchanger regulates cytolysin/perforin-induced increases in intracellular $Ca^{2+}$ and susceptibility to cytolysis. J. Immunol. **148:**2489–2496.
27. **Laemmli, U. K.** 1970. Cleavage of structural proteins during the assembly of the head of bacteriophage T4. Nature (London) **227:**680–685.
28. **LaVallie, E. R., E. A. DiBlasio, S. Kovacic, K. L. Grant, P. F. Schendel, and J. M. McCoy.** 1992. A thioredoxin gene fusion expression system that circumvents inclusion body formation in *E. coli* cytoplasm. Bio/Technology **11:**187–193.
29. **Ludwig, A., T. Jarchau, R. Benz, and W. Goebel.** 1988. The repeat domain of *Escherichia coli* haemolysin (HlyA) is responsible for its $Ca^{2+}$-dependent binding to erythrocytes. Mol. Gen. Genet. **214:**553–561.
30. **Lutz, F., M. Monhr, M. Grimmig, R. Leidolf, and D. Linder.** 1993. *Pseudomonas aeruginosa* cytotoxin-binding protein in rabbit erythrocyte membranes. An oligomer of 28 kDa with similarity to transmembrane channel proteins. Eur. J. Biochem. **217:**1123–1128.
31. **Miyake, M., T. Honda, and T. Miwatani.** 1989. Effects of divalent cations and saccharides on *Vibrio metschnikovii* cytolysin-induced hemolysis of rabbit erythrocytes. Infect. Immun. **57:**158–163.
32. **Nakamura, M., N. Sekino, M. Iwamoto, and Y. Ohno-Iwashita.** 1995. Interaction of Θ-toxin (perfringolysin O), a cholesterol-binding cytolysin, with liposomal membranes: change in the aromatic side chains upon binding and

insertion. Biochemistry **34:**6513–6520.
33. **Peterson, J. W., W. D. Dickey, S. S. Saini, W. Gourley, G. R. Klimpel, and A. K. Chopra.** 1996. Phospholipase $A_2$ activating protein and idiopathic inflammatory bowel disease. Gut **39:**698–704.
34. **Prasad, R., A. K. Chopra, P. Chary, and J. W. Peterson.** 1992. Expression and characterization of the cloned *Salmonella typhimurium* enterotoxin. Microb. Pathog. **13:**109–121.
35. **Reed, L. J., and H. Muench.** 1938. A simple method of estimating fifty percent endpoints. Am. J. Hyg. **27:**493–497.
36. **Rose, J. M., C. W. Houston, D. H. Coppenhaver, J. D. Dixon, and A. Kurosky.** 1989. Purification and chemical characterization of a cholera toxin-cross-reactive cytolytic enterotoxin produced by a human isolate of *Aeromonas hydrophila*. Infect. Immun. **57:**1165–1169.
37. **Rose, J. M., C. W. Houston, and A. Kurosky.** 1989. Bioactivity and immunological characterization of a cholera toxin-cross-reactive cytolytic enterotoxin from *Aeromonas hydrophila*. Infect. Immun. **57:**1170–1176.
38. **Sellman, B. R., B. L. Kagan, and R. K. Tweten.** 1997. Generation of a membrane-bound, oligomerized pre-pore complex is necessary for pore formation by *Clostridium septicum* alpha toxin. Mol. Microbiol. **23:**551–558.
39. **Song, L., M. R. Hobaugh, C. Shustak, S. Cheley, H. Bayley, and J. E. Gouaux.** 1996. Structure of staphylococcal α-hemolysin, a heptameric transmembrane pore. Science **274:**1805–1976.
40. **Tabor, S., and C. C. Richardson.** 1985. A bacteriophage T7 RNA polymerase/promoter system for controlled exclusive expression of specific genes. Proc. Natl. Acad. Sci. USA **82:**1074–1078.
41. **van Leengoed, L. A. M. G., and H. W. Dickerson.** 1992. Influence of calcium on secretion and activity of the cytolysins of *Actinobacillus pleuropneumoniae*. Infect. Immun. **60:**353–359.
42. **Yamamoto, K., Y. Ichinose, H. Shinagawa, K. Makino, A. Nakata, M. Iwanaga, T. Honda, and T. Miwatani.** 1990. Two-step processing for activation of the cytolysin/hemolysin of *Vibrio cholerae* O1 biotype El Tor: nucleotide sequence of the structural gene (*hlyA*) and characterization of the processed products. Infect. Immun. **58:**4106–4116.
43. **Zitzer, A., I. Walev, M. Palmer, and S. Bhakdi.** 1995. Characterization of *Vibrio cholerae* El Tor cytolysin as an oligomerizing pore-forming toxin. Med. Microbiol. Immunol. **184:**37–44.

*Editor:* J. T. Barbieri